Journal of Materials Science & Nanotechnology
Volume 9 | Issue 1
ISSN: 2348-9812

Research Article Open Access

On Optimization of Manufacturing of Field-Effect Heterotransistors Framework Current Comparator to Increase their Density

Pankratov EL[*1,2]

[1]Nizhny Novgorod State University, 23 Gagarin Avenue, Nizhny Novgorod, 603950, Russia
[2]Nizhny Novgorod State Technical University, 24 Minin Street, Nizhny Novgorod, 603950, Russia

[*]**Corresponding author:** Pankratov EL, Nizhny Novgorod State University, 23 Gagarin Avenue, and Nizhny Novgorod State Technical University, 24 Minin Street, Nizhny Novgorod, 603950, Russia, E-mail: elp2004@mail.ru

Citation: Pankratov EL (2020) On Optimization of Manufacturing of Field-Effect Heterotransistors Framework Current Comparator to Increase their Density. J Mater Sci Nanotechnol 9(1): 101

Received Date: January 20, 2021 Accepted Date: May 20, 2021 Published Date: May 22, 2021

Abstract

In this paper we introduce an analytical approach to analyze mass and heat transport in heterostructures during manufacturing of integrated circuits with account nonlinearity of processes. The approach gives a possibility to analyze mass and heat transport in multilayer structures without crosslinking of solutions on interfaces between layers. The approach also gives a possibility to take into account spatial and temporal variation of parameters of considered processes. Based on this approach we analyzed manufacturing a current comparator to increase density of elements.

Keywords: Current Comparator; Optimization of Manufacturing; Analytical Approach for Modelling

Introduction

An actual and intensively solving problems of solid state electronics is increasing of integration rate of elements of integrated circuits (*p*-*n*-junctions, their systems et al.) [1-8]. Increasing of the integration rate leads to necessity to de-crease their dimensions. To decrease the dimensions are using several approaches. They are widely using laser and mi-crowave types of annealing of infused dopants. These types of annealing are also widely using for annealing of radia-tion defects, generated during ion implantation [9-17]. Using the approaches gives a possibility to increase integration rate of elements of integrated circuits through inhomogeneity of technological parameters due to generating inhomoge-nous distribution of temperature. In this situation one can obtain decreasing dimensions of elements of integrated cir-cuits [18] with account Arrhenius law [1,3]. Another approach to manufacture elements of integrated circuits with smaller dimensions is doping of heterostructure by diffusion or ion implantation [1-3]. However in this case optimiza-tion of dopant and/or radiation defects is required [18].

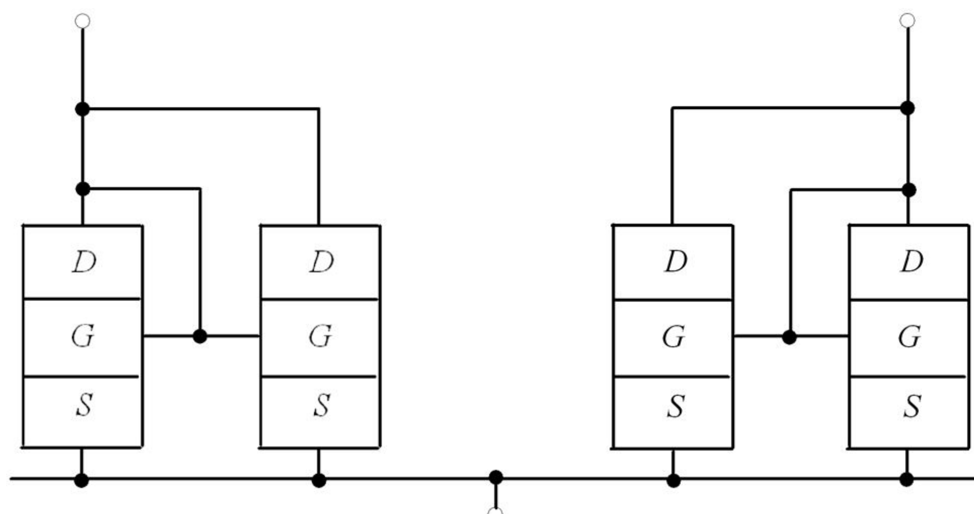

Figure 1: The considered current comparator [4]

In this paper we consider a heterostructure. The heterostructure consist of a substrate and several epitaxial layers. Some sections have been manufactured in the epitaxial layers. Further we consider doping of these sections by diffusion or ion implantation. The doping gives a possibility to manufacture field-effect transistors framework a cascaded-inverter circuit so as it is shown on Figure 1. The manufacturing gives a possibility to increase density of elements of the considered in [4] current comparator. After the considered doping dopant and/or radiation defects should be annealed. Framework the paper we analyzed dynamics of redistribution of dopant and/or radiation defects during their annealing. We introduce an approach to decrease dimensions of the element. However it is necessary to complicate technological process.

Method of solution

In this section we determine spatio-temporal distributions of concentrations of infused and implanted dopants. To determine these distributions we calculate appropriate solutions of the second Fick's law [1,3,18]

$$\frac{\partial C(x,y,z,t)}{\partial t}=$$

$$=\frac{\partial}{\partial x}\left[D_C\frac{\partial C(x,y,z,t)}{\partial x}\right]+\frac{\partial}{\partial y}\left[D_C\frac{\partial C(x,y,z,t)}{\partial y}\right]+\frac{\partial}{\partial z}\left[D_C\frac{\partial C(x,y,z,t)}{\partial z}\right]. \quad (1)$$

Boundary and initial conditions for the equations are

$$\left.\frac{\partial C(x,y,z,t)}{\partial x}\right|_{x=0}=0\quad \left.\frac{\partial C(x,y,z,t)}{\partial x}\right|_{x=L_x}=0\quad \left.\frac{\partial C(x,y,z,t)}{\partial y}\right|_{y=0}=0\quad \left.\frac{\partial C(x,y,z,t)}{\partial y}\right|_{x=L_y}=0,$$

$$\left.\frac{\partial C(x,y,z,t)}{\partial z}\right|_{z=0}=0\quad \left.\frac{\partial C(x,y,z,t)}{\partial z}\right|_{x=L_z}=0\quad , C(x,y,z,0)=f(x,y,z). \quad (2)$$

The function $C(x,y,z,t)$ describes the spatio-temporal distribution of concentration of dopant; T is the temperature of annealing; D_C is the dopant diffusion coefficient. Value of dopant diffusion coefficient could be changed with changing materials of heterostructure, with changing temperature of materials (including annealing), with changing concentrations of dopant and radiation defects. We approximate dependences of dopant diffusion coefficient on parameters by the following relation with account results in Refs. [20-22]

$$D_C=D_L(x,y,z,T)\left[1+\xi\frac{C^\gamma(x,y,z,t)}{P^\gamma(x,y,z,T)}\right]\left[1+\varsigma_1\frac{V(x,y,z,t)}{V^*}+\varsigma_2\frac{V^2(x,y,z,t)}{(V^*)^2}\right]. \quad (3)$$

Here the function $D_L(x,y,z,T)$ describes the spatial (in heterostructure) and temperature (due to Arrhenius law) depend-ences of diffusion coefficient of dopant. The function $P(x,y,z,T)$ describes the limit of solubility of dopant. Parameter γε[1,3] describes average quantity of charged defects interacted with atom of dopant [20]. The function $V(x,y,z,t)$ de-scribes the spatio-temporal distribution of concentration of radiation vacancies. Parameter V^* describes the equilibrium distribution of concentration of vacancies. The considered concentrational dependence of dopant diffusion coefficient has been described in details in [20]. It should be noted, that using diffusion type of doping did not generation radiation defects. In this situation $\zeta_1=\zeta_2=0$. We determine spatio-temporal distributions of concentrations of radiation defects by solving the following system of equations [21,22]

$$\frac{\partial I(x,y,z,t)}{\partial t}=\frac{\partial}{\partial x}\left[D_I(x,y,z,T)\frac{\partial I(x,y,z,t)}{\partial x}\right]+\frac{\partial}{\partial y}\left[D_I(x,y,z,T)\frac{\partial I(x,y,z,t)}{\partial y}\right]+$$

$$+\frac{\partial}{\partial z}\left[D_I(x,y,z,T)\frac{\partial I(x,y,z,t)}{\partial z}\right]-k_{I,V}(x,y,z,T)\,I(x,y,z,t)\,V(x,y,z,t)-$$

$$-k_{I,I}(x,y,z,T)I^2(x,y,z,t) \quad (4)$$

$$\frac{\partial V(x,y,z,t)}{\partial t}=\frac{\partial}{\partial x}\left[D_V(x,y,z,T)\frac{\partial V(x,y,z,t)}{\partial x}\right]+\frac{\partial}{\partial y}\left[D_V(x,y,z,T)\frac{\partial V(x,y,z,t)}{\partial y}\right]+$$

$$+\frac{\partial}{\partial z}\left[D_V(x,y,z,T)\frac{\partial V(x,y,z,t)}{\partial z}\right]-k_{I,V}(x,y,z,T)I(x,y,z,t)\;V(x,y,z,t)+$$

$$+k_{V,V}(x,y,z,T)V^2(x,y,z,t).$$

Boundary and initial conditions for these equations are

$$\left.\frac{\partial \rho(x,y,z,t)}{\partial x}\right|_{x=0}=0,\quad \left.\frac{\partial \rho(x,y,z,t)}{\partial x}\right|_{x=L_x}=0,\quad \left.\frac{\partial \rho(x,y,z,t)}{\partial y}\right|_{y=0}=0,\quad \left.\frac{\partial \rho(x,y,z,t)}{\partial y}\right|_{y=L_y}=0,$$

$$\left.\frac{\partial \rho(x,y,z,t)}{\partial z}\right|_{z=0}=0,\quad \left.\frac{\partial \rho(x,y,z,t)}{\partial z}\right|_{z=L_z}=0,\quad P\,(x,y,z,0)=fp\,(x,y,z). \tag{5}$$

Here $p=I,V$. The function $I\,(x,y,z,t)$ describes the spatio-temporal distribution of concentration of radiation intersti-tials; $D_p(x,y,z,T)$ are the diffusion coefficients of point radiation defects; terms $V^2(x,y,z,t)$ and $I^2(x,y,z,t)$ correspond to generation divacancies and diinterstitials; $k_{I,V}(x,y,z,T)$ is the parameter of recombination of point radiation defects; $k_{I,I}(x,y,z,T)$ and $k_{V,V}(x,y,z,T)$ are the parameters of generation of simplest complexes of point radiation defects.

Further we determine distributions in space and time of concentrations of divacancies $\Phi_V(x,y,z,t)$ and diinterstitials $\Phi_I(x,y,z,t)$ by solving the following system of equations [21,22]

$$\frac{\partial \Phi_I(x,y,z,t)}{\partial t}=\frac{\partial}{\partial x}\left[D_{\Phi I}(x,y,z,T)\frac{\partial \Phi_I(x,y,z,t)}{\partial x}\right]+\frac{\partial}{\partial y}\left[D_{\Phi I}(x,y,z,T)\frac{\partial \Phi_I(x,y,z,t)}{\partial y}\right]+$$

$$+\frac{\partial}{\partial z}\left[D_{\Phi I}(x,y,z,T)\frac{\partial \Phi_I(x,y,z,t)}{\partial z}\right]+k_{I,I}(x,y,z,T)I^2(x,y,z,t)-k_I(x,y,z,T)I(x,y,z,t)$$

$$\frac{\partial \Phi_V(x,y,z,t)}{\partial t}=\frac{\partial}{\partial x}\left[D_{\Phi V}(x,y,z,T)\frac{\partial \Phi_V(x,y,z,t)}{\partial x}\right]+\frac{\partial}{\partial y}\left[D_{\Phi V}(x,y,z,T)\frac{\partial \Phi_V(x,y,z,t)}{\partial y}\right]+$$

$$+\frac{\partial}{\partial z}\left[D_{\Phi V}(x,y,z,T)\frac{\partial \Phi_V(x,y,z,t)}{\partial z}\right]+k_{V,V}(x,y,z,T)V^2(x,y,z,t)-k_V(x,y,z,T)V(x,y,z,t).$$

Boundary and initial conditions for these equations are

$$\left.\frac{\partial \Phi_\rho(x,y,z,t)}{\partial x}\right|_{x=0}=0,\quad \left.\frac{\partial \Phi_\rho(x,y,z,t)}{\partial x}\right|_{x=L_x}=0,\quad \left.\frac{\partial \Phi_\rho(x,y,z,t)}{\partial y}\right|_{y=0}=0,\quad \left.\frac{\partial \Phi_\rho(x,y,z,t)}{\partial y}\right|_{y=L_y}=0,$$

$$\left.\frac{\partial \Phi_\rho(x,y,z,t)}{\partial z}\right|_{z=0}=0,\quad \left.\frac{\partial \Phi_\rho(x,y,z,t)}{\partial z}\right|_{z=L_z}=0,$$

$\Phi_I\,(x,y,z,0)=f_{\Phi I}\,(x,y,z)$, $\Phi V\,(x,y,z,0)=f_{\Phi V}\,(x,y,z)$. (7)

Here $D_{\Phi\rho}(x,y,z,T)$ are the diffusion coefficients of the above complexes of radiation defects; $k_I(x,y,z,T)$ and $k_V\,(x,y,z,T)$ are the parameters of decay of these complexes.

We calculate distributions of concentrations of point radiation defects in space and time by recently elaborated ap-proach [18]. The approach based on transformation of approximations of diffusion coefficients in the following form: $D_\rho(x,y,z,T)=D_{0\rho}[1+\varepsilon_\rho g_\rho(x,y,z,T)]$, where $D_{0\rho}$ are the average values of diffusion coefficients, $0\le\varepsilon_\rho<1$, $|g_\rho(x, y,z,T)|\le1$, $\rho=I,V$. We also used analogous transformation of approximations of parameters of recombination of point defects and parameters of generation of their complexes: $k_{I,V}(x,y,z,T)=k_{0I,V}[1+\varepsilon_{I,V}\, g_{I,V}(x,y,z,T)]$, $k_{I,I}(x,y,z,T)=k_{0I,I}\,[1+\varepsilon_{I,I}\, g_{I,I}(x,y,z,T)]$ and $k_{V,V}(x,y,z,T)=k_{0V,V}\,[1+\varepsilon_{V,V}\, g_{V,V}(x,y,z,T)]$, where $k_{0\rho1,\rho2}$ are the their average values, $0\le\varepsilon_{I,V}<1$, $0\le\varepsilon_{I,I}<1$, $0\le\varepsilon_{V,V}<1$, $|g_{I,V}(x,y,z,T)|\le1$, $|g_{I,I}(x,y,z,T)|\le1$, $|g_{V,V}(x,y,z,T)|\le1$. Let us introduce the following dimensionless variables:

$$\tilde{I}(x,y,z,t)=I(x,y,z,t)/I^*,\quad \tilde{V}(x,y,z,t)= \;=V(x,y,z,t)/V^*,\quad \omega=L^2k_{0I,V}\Big/\sqrt{D_{0I}D_{0V}},$$

$$\Omega_\rho=L^2k_{0\rho,\rho}\Big/\sqrt{D_{0I}D_{0V}},\quad \vartheta=\sqrt{D_{0I}D_{0V}}\,t/L^2,\quad \chi = x/Lx,\ \eta = y/Ly,\ \Phi = z/Lz.$$

The introduction leads to transformation of Eqs.(4) and conditions (5) to the following form

$$\frac{\partial\tilde{I}(\chi,\eta,\varphi,\vartheta)}{\partial\vartheta}=\frac{D_{0I}}{\sqrt{D_{0I}D_{0V}}}\frac{\partial}{\partial\chi}\left\{\left[1+\varepsilon_I g_I(\chi,\eta,\varphi,T)\right]\frac{\partial\tilde{I}(\chi,\eta,\varphi,\vartheta)}{\partial\chi}\right\}+\frac{\partial}{\partial\eta}\left\{\left[1+\varepsilon_I g_I(\chi,\eta,\varphi,T)\right]\times\right.$$
$$\left.\times\frac{\partial\tilde{I}(\chi,\eta,\varphi,\vartheta)}{\partial\eta}\right\}\frac{D_{0I}}{\sqrt{D_{0I}D_{0V}}}+\frac{D_{0I}}{\sqrt{D_{0I}D_{0V}}}\frac{\partial}{\partial\varphi}\left\{\left[1+\varepsilon_I g_I(\chi,\eta,\varphi,T)\right]\frac{\partial\tilde{I}(\chi,\eta,\varphi,\vartheta)}{\partial\varphi}\right\}-\tilde{I}(\chi,\eta,\varphi,\vartheta)\times$$
$$\times\omega\left[1+\varepsilon_{I,V}g_{I,V}(\chi,\eta,\varphi,T)\right]\tilde{V}(\chi,\eta,\varphi,\vartheta)-\Omega_I\left[1+\varepsilon_{I,I}g_{I,I}(\chi,\eta,\varphi,T)\right]\tilde{I}^2(\chi,\eta,\varphi,\vartheta) \qquad (8)$$

$$\frac{\partial\tilde{V}(\chi,\eta,\varphi,\vartheta)}{\partial\vartheta}=\frac{D_{0V}}{\sqrt{D_{0I}D_{0V}}}\frac{\partial}{\partial\chi}\left\{\left[1+\varepsilon_V g_V(\chi,\eta,\varphi,T)\right]\frac{\partial\tilde{V}(\chi,\eta,\varphi,\vartheta)}{\partial\chi}\right\}+\frac{\partial}{\partial\eta}\left\{\left[1+\varepsilon_V g_V(\chi,\eta,\varphi,T)\right]\times\right.$$
$$\left.\times\frac{\partial\tilde{V}(\chi,\eta,\varphi,\vartheta)}{\partial\eta}\right\}\frac{D_{0V}}{\sqrt{D_{0I}D_{0V}}}+\frac{D_{0V}}{\sqrt{D_{0I}D_{0V}}}\frac{\partial}{\partial\varphi}\left\{\left[1+\varepsilon_V g_V(\chi,\eta,\varphi,T)\right]\frac{\partial\tilde{V}(\chi,\eta,\varphi,\vartheta)}{\partial\varphi}\right\}-\tilde{I}(\chi,\eta,\varphi,\vartheta)\times$$
$$\times\omega\left[1+\varepsilon_{I,V}g_{I,V}(\chi,\eta,\varphi,T)\right]\tilde{V}(\chi,\eta,\varphi,\vartheta)-\Omega_V\left[1+\varepsilon_{V,V}g_{V,V}(\chi,\eta,\varphi,T)\right]\tilde{V}^2(\chi,\eta,\varphi,\vartheta)$$

$$\left.\frac{\partial\tilde{\rho}(\chi,\eta,\varphi,\vartheta)}{\partial\chi}\right|_{\chi=0}=0,\quad \left.\frac{\partial\tilde{\rho}(\chi,\eta,\varphi,\vartheta)}{\partial\chi}\right|_{\chi=1}=0,\quad \left.\frac{\partial\tilde{\rho}(\chi,\eta,\varphi,\vartheta)}{\partial\eta}\right|_{\eta=0}=0,\quad \left.\frac{\partial\tilde{\rho}(\chi,\eta,\varphi,\vartheta)}{\partial\eta}\right|_{\eta=1}=0,$$

$$\left.\frac{\partial\tilde{\rho}(\chi,\eta,\varphi,\vartheta)}{\partial\varphi}\right|_{\varphi=0}=0,\quad \left.\frac{\partial\tilde{\rho}(\chi,\eta,\varphi,\vartheta)}{\partial\varphi}\right|_{\varphi=1}=0,\quad \tilde{\rho}(\chi,\eta,\varphi,\vartheta)=\frac{f_\rho(\chi,\eta,\varphi,\vartheta)}{\rho^*}. \qquad (9)$$

We determine solutions of Eqs.(8) with conditions (9) framework recently introduced approach [18], i.e. as the power series

$$\tilde{\rho}(\chi,\eta,\varphi,\vartheta)=\sum_{i=0}^{\infty}\varepsilon_\rho^i\sum_{j=0}^{\infty}\omega^j\sum_{k=0}^{\infty}\Omega_\rho^k\tilde{\rho}_{ijk}(\chi,\eta,\varphi,\vartheta). \qquad (10)$$

Substitution of the series (10) into Eqs.(8) and conditions (9) gives us possibility to obtain equations for initial-order approximations of concentration of point defects $\tilde{I}_{000}(\chi,\eta,\varphi,\vartheta)$ and $\tilde{V}_{000}(\chi,\eta,\varphi,\vartheta)$ and corrections for them $\tilde{I}_{ijk}(\chi,\eta,\varphi,\vartheta)$ and $\tilde{V}_{ijk}(\chi,\eta,\varphi,\vartheta)$, $i\ge1$, $j\ge1$, $k\ge1$. The equations are presented in the Appendix. Solutions of the equations could be obtained by standard Fourier approach [24,25]. The solutions are presented in the Appendix.

Now we calculate distributions of concentrations of simplest complexes of point radiation defects in space and time. To determine the distributions we transform approximations of diffusion coefficients in the following form: $D_{\Phi\rho}(x,y,z,T)=D_{0\Phi\rho}[1+\varepsilon_{\Phi\rho}g_{\Phi\rho}(x,y,z,T)]$, where $D0_{\Phi\rho}$ are the average values of diffusion coefficients. In this situation the Eqs.(6) could be written as

$$\frac{\partial\,\Phi_I(x,y,z,t)}{\partial\,t}=D_{0\Phi I}\frac{\partial}{\partial x}\left\{\left[1+\varepsilon_{\Phi I}g_{\Phi I}(x,y,z,T)\right]\frac{\partial\Phi_I(x,y,z,t)}{\partial x}\right\}+k_{I,I}(x,y,z,T)\,I^2(x,y,z,t)+$$

$$+D_{0\Phi I}\frac{\partial}{\partial\,y}\left\{\left[1+\varepsilon_{\Phi I}g_{\Phi I}(x,y,z,T)\right]\frac{\partial\Phi_I(x,y,z,t)}{\partial\,y}\right\}+D_{0\Phi I}\frac{\partial}{\partial\,z}\left\{\left[1+\varepsilon_{\Phi I}g_{\Phi I}(x,y,z,T)\right]\frac{\partial\Phi_I(x,y,z,t)}{\partial z}\right\}-$$

$$-k_I(x,y,z,T)\,I(x,y,z,t)$$

$$\frac{\partial\,\Phi_V(x,y,z,t)}{\partial\,t}=D_{0\Phi V}\frac{\partial}{\partial x}\left\{\left[1+\varepsilon_{\Phi V}g_{\Phi V}(x,y,z,T)\right]\frac{\partial\Phi_V(x,y,z,t)}{\partial x}\right\}+k_{I,I}(x,y,z,T)\,I^2(x,y,z,t)+$$

$$+D_{0\Phi V}\frac{\partial}{\partial\,y}\left\{\left[1+\varepsilon_{\Phi V}g_{\Phi V}(x,y,z,T)\right]\frac{\partial\Phi_V(x,y,z,t)}{\partial\,y}\right\}+D_{0\Phi V}\frac{\partial}{\partial\,z}\left\{\left[1+\varepsilon_{\Phi V}g_{\Phi V}(x,y,z,T)\right]\frac{\partial\Phi_V(x,y,z,t)}{\partial z}\right\}-$$

$$-k_I(x,y,z,T)\,I(x,y,z,t)\,.$$

Farther we determine solutions of above equations as the following power series

$$\Phi_\rho(x,y,z,t)=\sum_{i=0}^{\infty}\varepsilon_{\Phi\rho}^i\Phi_{\rho i}(x,y,z,t). \qquad (11)$$

Now we used the series (11) into Eqs.(6) and appropriate boundary and initial conditions. The using gives the pos-sibility to obtain equations for initial-order approximations of concentrations of complexes of defects $\Phi_{\rho 0}(x,y,z,t)$, cor-rections for them $\Phi_{\rho i}(x,y,z,t)$ (for them $i \geq 1$) and boundary and initial conditions for them. We remove equations and conditions to the Appendix. Solutions of the equations have been calculated by standard approaches [24,25] and pre-sented in the Appendix.

Now we calculate distribution of concentration of dopant in space and time by using the approach, which was used for analysis of radiation defects. To use the approach we consider following transformation of approximation of dopant diffusion coefficient: $D_L(x,y,z,T)=D_{0L}[1+\varepsilon_L g_L(x,y,z,T)]$, where D0L is the average value of dopant diffusion coefficient, $0\leq\varepsilon_L< 1$, $|g_L(x,y,z,T)|\leq 1$. Farther we consider solution of Eq.(1) as the following series:

$$C(x,y,z,t)=\sum_{i=0}^{\infty}\varepsilon_L^i\sum_{j=1}^{\infty}\xi^j C_{ij}(x,y,z,t) \qquad (11)$$

Using the relation into Eq.(1) and conditions (2) leads to obtaining equations for the functions Cij(x,y,z,t) (i ≥1, j ≥1), boundary and initial conditions for them. The equations are presented in the Appendix. Solutions of the equations have been calculated by standard approaches (see, for example, [24,25]). The solutions are presented in the Appendix.

We analyzed distributions of concentrations of dopant and radiation defects in space and time analytically by using the second-order approximations on all parameters, which have been used in appropriate series. Usually the second-order approximations are enough good approximations to make qualitative analysis and to obtain quantitative results. All analytical results have been checked by numerical simulation.

Discussion

In this section we analyzed calculated in previous section the spatio-temporal distributions of concentrations of do-pants. Figure 2 shows typical spatial distributions of concentrations of dopants in neighborhood of interfaces between layers of heterostructures. We calculate the above distributions of concentrations of dopants under the following condi-tion: value of dopant diffusion coefficient in doped area is larger, than values of dopant diffusion coefficient in nearest areas. In this situation one can find increasing of compactness of dopant in the heterostructure (Figure 2). At the same time one can find increasing of homogeneity of distribution of concentration of dopant (Figure 2). The first of the above effects gives a possibility to decrease dimensions of field-effect transistors and at the same time to increase their density. The second effect gives a possibility to decrease local overheats during functioning of these transistors or to decrease dimensions of the above transistors with fixed value of these overheats. Changing relation between values of dopant diffusion coefficients leads to opposite result (Figure 3).

It should be noted, that framework the considered approach one shall optimize annealing of dopant and/or radiation defects. Reason of the optimization is following. Increasing of annealing time leads to obtaining of too homogenous spatial distribution of concentration of dopant with decreasing of difference between doped and undoped areas of heterostructure. Decreasing of annealing time leads to obtaining of too homogenous spatial distribution of concentration of dopant with increasing local overheats during functioning of transistors. In this situation it is attracted an interest choosing of compromised value of annealing time. To estimate the compromised value of annealing time we used recently introduced criterion [26-33]. The choosing based on approximation real distribution by step-wise function Ψ (x,y,z) (Figure 4). Farther the required values of optimal annealing time have been calculated by mini-mization the following mean-squared error.

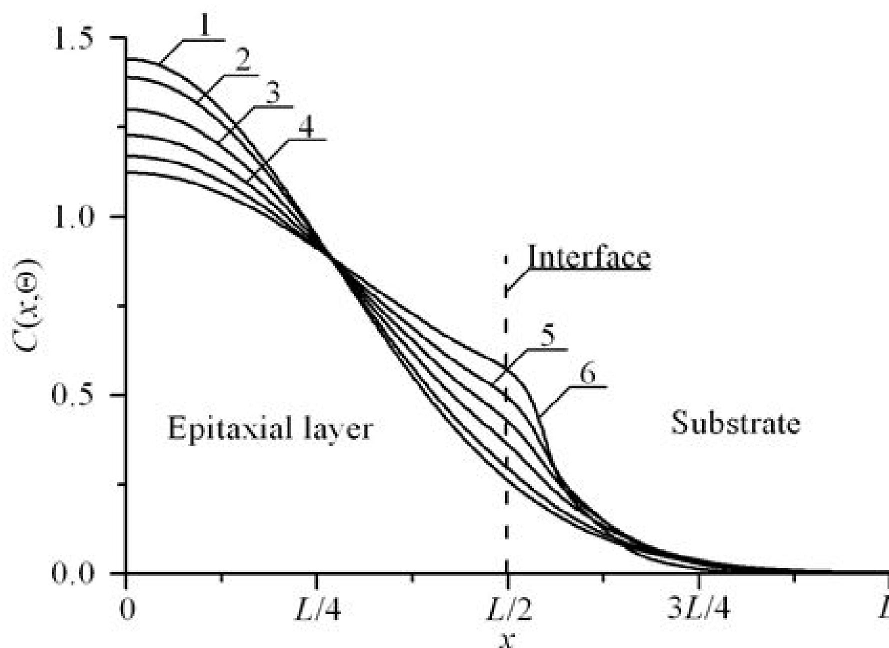

Figure 2a: Dependences of concentration of dopant, infused in heterostructure from Figure 1, on coordinate in direc-tion, which is perpendicular to interface between epitaxial layer substrate. Difference between values of dopant diffu-sion coefficient in layers of heterostructure increases with increasing of number of curves. Value of dopant diffusion coefficient in the epitaxial layer is larger, than value of dopant diffusion coefficient in the substrate.

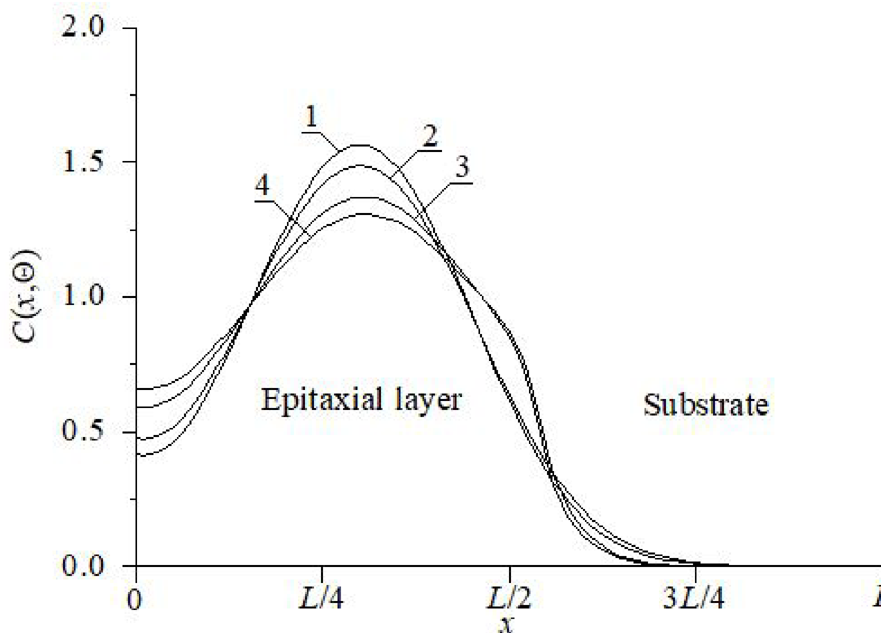

Figure 2b: Dependences of concentration of dopant, implanted in heterostructure from Figure 1, on coordinate in direction, which is perpendicular to interface between epitaxial layer substrate. Difference between values of dopant diffusion coefficient in layers of heterostructure increases with increasing of number of curves. Value of dopant diffusion coefficient in the epitaxial layer is larger, than value of dopant diffusion coefficient in the substrate. Curve 1 corresponds to homogenous sample and annealing time $\Theta = 0.0048$ $(L_x^2+L_y^2+L_z^2)/D_0$. Curve 2 corresponds to homogenous sample and annealing time $\Theta = 0.0057$ $(L_x^2+L_y^2+L_z^2)/D_0$. Curves 3 and 4 correspond to heterostructure from Figure 1; annealing times $\Theta = 0.0048$ $(L_x^2+L_y^2+L_z^2)/D_0$ and $\Theta = 0.0057$ $(L_x^2+L_y^2+L_z^2)/D_0$, respectively

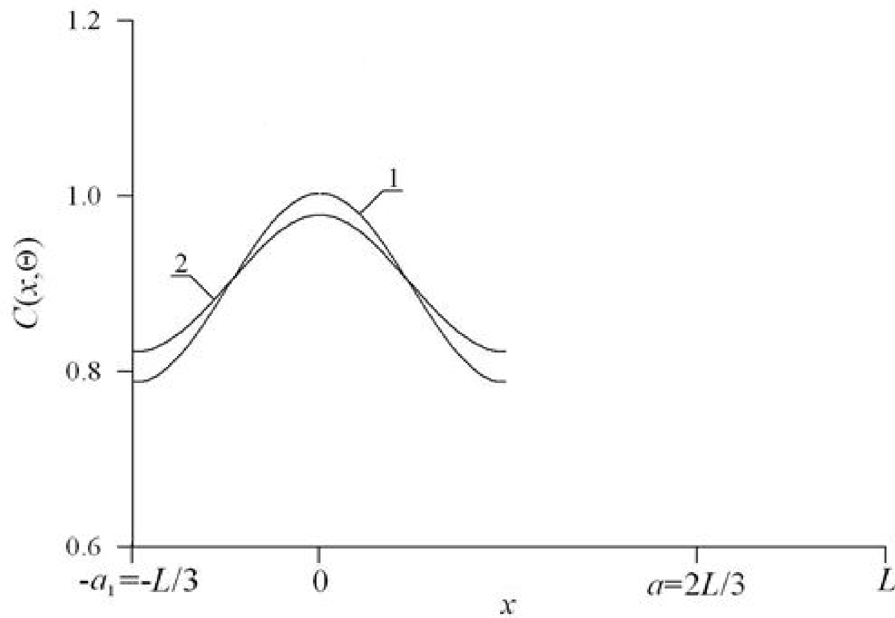

Figure 3a: Distributions of concentration of dopant, infused in average section of epitaxial layer of heterostructure from Figure 1 in direction parallel to interface between epitaxial layer and substrate of heterostructure. Difference between values of dopant diffusion coefficients increases with increasing of number of curves. Value of dopant diffusion coefficient in this section is smaller, than value of dopant diffusion coefficient in nearest sections.

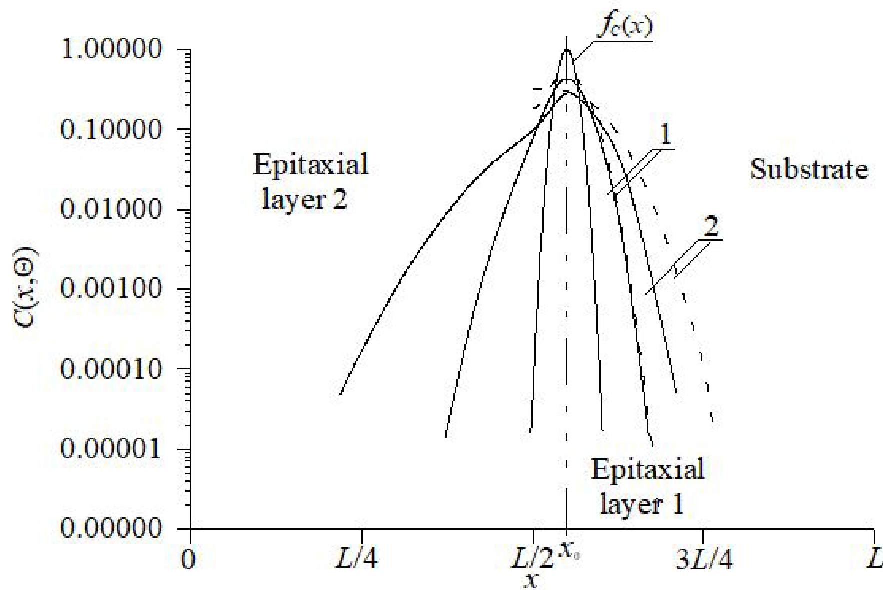

Figure 3b: Calculated distributions of implanted dopant in epitaxial layers of heterostructure. Solid lines are spatial distributions of implanted dopant in system of two epitaxial layers. Dushed lines are spatial distributions of implanted dopant in one epitaxial layer. Annealing time increases with increasing of number of curves

$$U=\frac{1}{L_xL_yL_z}\int_0^{L_x}\int_0^{L_y}\int_0^{L_z}\left[C(x,y,z,\Theta)-\psi(x,y,z)\right]d\,z\,d\,y\,d\,x. \tag{13}$$

We show optimal values of annealing time as functions of parameters on Figure 5. It is known, that standard step of manufactured ion-doped structures is annealing of radiation defects. In the ideal case after finishing the annealing dopant achieves interface between layers of heterostructure. If the dopant has no enough time to achieve the interface, it is practicably to anneal the dopant additionally. The Figure 5b shows the described dependences of optimal values of additional annealing time for the same parameters as for Figure 5a. Necessity to anneal radiation defects leads to smaller values of optimal annealing of implanted dopant in comparison with optimal annealing time of infused dopant. Curves 1 on Figure 5 describe dependences of the annealing time on the relation a/L and $\xi = \gamma = 0$ for equal to each other values of dopant diffusion coefficient in all parts of heterostructure. These dependences could be qualitatively explained by increasing of thickness of epitaxial layer. The increasing leads to increasing

of time of achievement of interface between layers of heterostructure. Curves 2 describe the dependence of the annealing time on value of parameter ε for a/L=1/2 and $\xi = \gamma = 0$. Increasing of parameter ε leads to increasing of difference between values of dopant diffusion coefficient in doped and undoped areas. The increasing leads to decreasing of speed of dopant diffusion in undoped area with increasing of of optimal value of annealing time. Curves 3 describes the dependence of the annealing time on value of parameter ξ for a/L=1/2 and $\varepsilon = \gamma = 0$. Increasing of value of parameter ξ leads to increasing of the second term of approximation of dopant diffusion coefficient. The increasing leads to increasing of dopant diffusion coefficient and increasing of speed of dopant. The increasing of speed of dopant leads to decreasing of value of compromise value of annealing time. Curves 4 describes the dependence of the annealing time on value of parameter γ for a/L=1/2 and ε = ξ = 0. Increasing of value of parameter leads to increasing of the second term of approximation of dopant diffusion coefficient. The increasing leads to increasing of dopant diffusion coefficient and increasing of speed of dopant. The increasing of speed of dopant leads to decreasing of value of compromise value of annealing time.

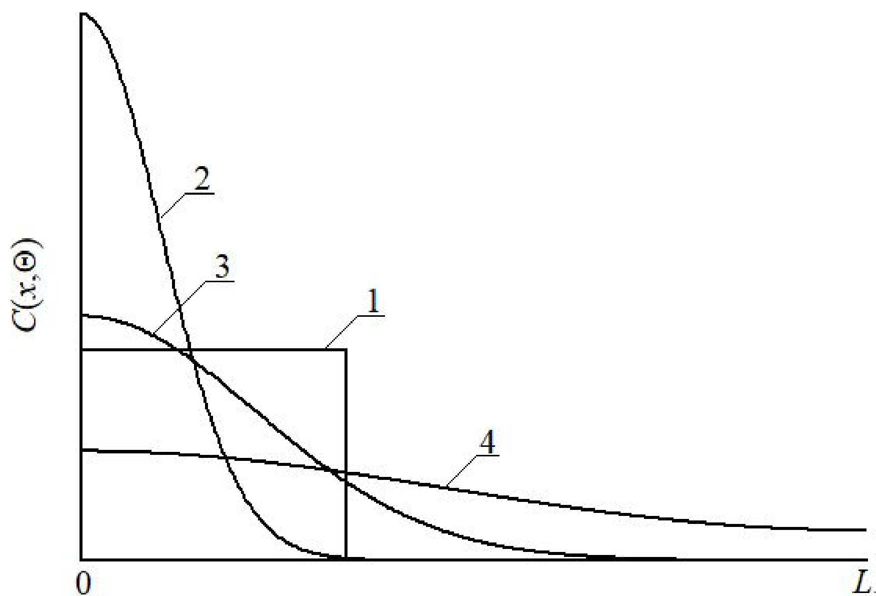

Figure 4a: Distributions of concentration of infused dopant in depth of heterostructure from Figure 1 for different val-ues of annealing time (curves 2-4) and idealized step-wise approximation (curve 1). Increasing of number of curve cor-responds to increasing of annealing time

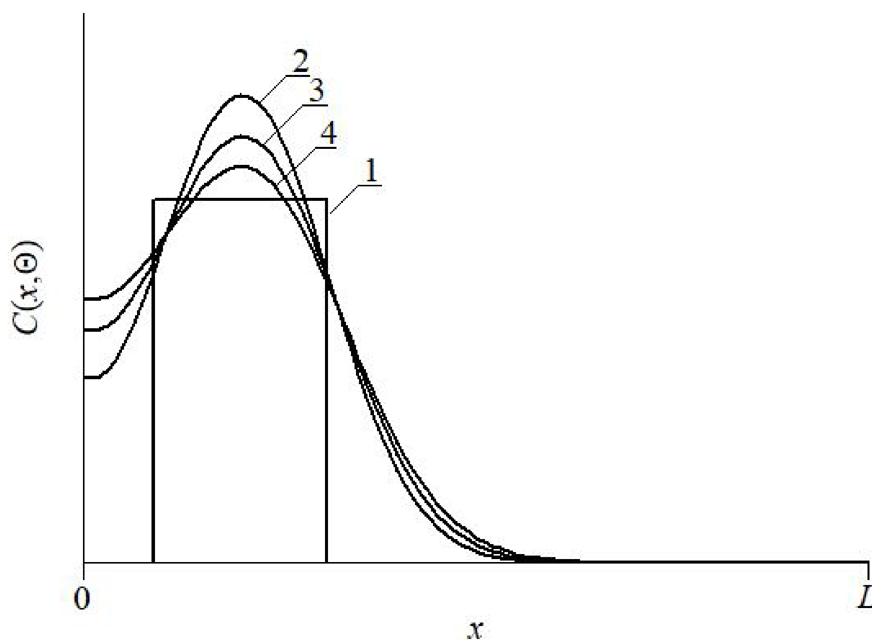

Figure 4b: Distributions of concentration of implanted dopant in depth of heterostructure from Figure 1 for different values of annealing time (curves 2-4) and idealized step-wise approximation (curve 1). Increasing of number of curve corresponds to increasing of annealing time

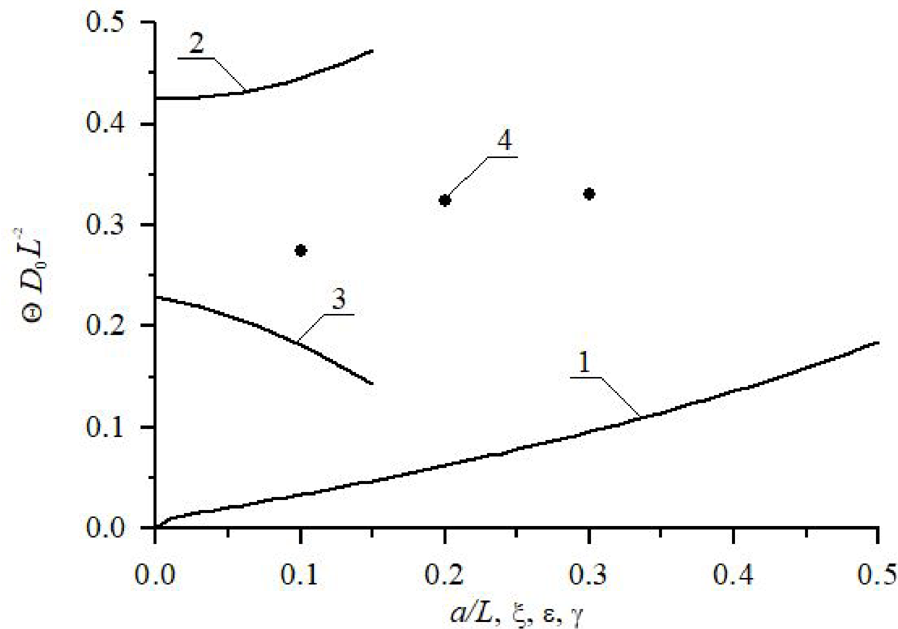

Figure 5a: Dimensionless optimal annealing time of infused dopant as a function of several parameters

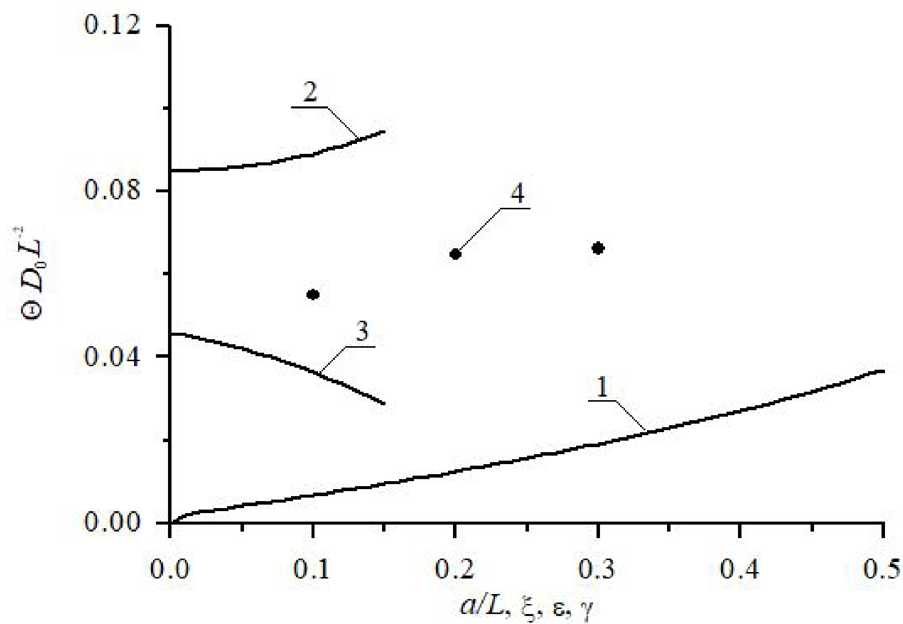

Figure 5b: Dimensionless optimal annealing time of implanted dopant as a function of several parameters

Conclusions

In this paper we introduce an approach to increase integration rate of element of a current comparator. The ap-proach gives us possibility to decrease area of the elements with smaller increasing of the element's thickness.

Appendix

References

1. Pankratov EL (2010) Optimization of Pulse Laser Annealing to Increase Sharpness of Implanted-junction Rectifier in Semiconductor Heterostructure. Nano-Micro Lett 2: 256-67.

2. Alexenko AG, Shagurin II (1990) Microcircuitry (Radio and communication, Moscow, 1990), Russia.

3. Avaev NA, Naumov Yu E, Frolkin VT (1991) Basis of microelectronics (Radio and communication, Moscow, 1991), Russia.

4. Baradaranrezaeii A, Shino O, Hadidi K (2015) An ultra high-speed high-resolution low-offset low-power voltage comparator with a reliable offset cancellation method for high-performance applications in 0.18 μm CMOS technology. Analog Integr Circ Sig Process 85: 181-92.

5. Fathi D, Forouzandeh B, Masoumi N (2009) New enhanced noise analysis in active mixers in nanoscale technolo-gies. Nano 4: 233-238.

6. Chachuli SA, Fasyar PNA, Soin N, Karim NM, Yusop N (2014) Pareto ANOVA analysis for CMOS 0.18 μm two -stage Op-amp. Mat Sci Sem Proc 24: 9-14.

7. Ageev AO, Belyaev AE, Boltovets NS, Ivanov VN, Konakova RV, et al. (2009) Au-TiBx–n-6H-SiC Schottky barrier diodes: the features of current flow in rectifying and nonrectifying contacts. Semiconductors 43: 897-903.

8. Li Z, Waldron J, Detchprohm T, Wetzel C, Karlicek RF, et al. (2013) Monolithic integration of light-emitting diodes and power metal-oxide-semiconductor channel high-electron-mobility transistors for light-emitting power integrated circuits in GaN on sapphire substrate. Appl Phys Lett 102: 10.1063/1.4807125.

9. Tsai J-H, Chiu S-Y, Lour W-S, Guo D-F (2009) High-performance InGaP/GaAs pnp δ-doped heterojunction bipolar transistor. Semiconductors 43: 971-4.

10. Alexandrov OV, Zakhar'in AO, Sobolev NA, Shek EI, Makoviychuk MM, et al. (1998) Formation of donor centers after annealing of dysprosium and holmium implanted silicon. Semiconductors 32: 1029-32.

11. Kumar MJ, Singh TV (2008) Quantum confinement effects in strained silicon MOSFETs. Int J Nanoscience 7: 81-4.

12. Sinsermsuksakul P, Hartman K, Kim SB, Heo J, Sun L, et al. (2013) Enhancing the efficiency of SnS solar cells via band-offset engineering with a zinc oxysulfide buffer layer. Appl Phys Lett 102: 053901-5.

13. Reynolds JG, Reynolds CL, Mohanta A, Muth JF, Rowe JE, et al. (2013) Shallow acceptor complexes in p-type ZnO. Appl Phys Lett 102: 152114-8.

14. Ong KK, Pey KL, Lee PS, Wee ATS, Wang XC, et al. (2006) Dopant distribution in the recrystallization transient at the maximum melt depth induced by laser annealing. Appl Phys Lett 89: 172111-4.

15. Wang HT, Tan LS, Chor EF (2006) Pulsed laser annealing of Be-implanted GaN. J Appl Phys 98: 094901-5.

16. Shishiyanu ST, Shishiyanu TS, Railyan SK (2002) Shallow p-n-junctions in Si prepared by pulse photon annealing. Semiconductors 36: 611-7.

17. Bykov Yu V, Yeremeev AG, Zharova NA, Plotnikov IV, Rybakov KI, et al. (2003) Diffusion processes in semi-conductor structures during microwave annealing. Radiophysics and Quantum Electronics 43: 836-43.

18. Pankratov EL, Bulaeva EA (2013) Doping of materials during manufacture p-n-junctions and bipolar transistors. Analytical approaches to model technological approaches and ways of optimization of distributions of dopants. Reviews in Theoretical Science 1: 58-82.

19. Erofeev Yu N (1989) Pulse devices, Russia.

20. Kozlivsky VV (2003) Modification of semiconductors by proton beams, Russia.

21. Gotra Z Yu (1991) Technology of microelectronic devices Radio and communication, Moscow, Russia.

22. Vinetskiy VL, Kholodar GA (1979) Radiative physics of semiconductors, Russia.

23. Fahey PM, Griffin PB, Plummer JD (1989) Point defects and dopant diffusion in sikicon. Rev Mod Phys 61: 289-388.

24. Tikhonov AN, Samarskii AA (1972) Equations of Mathematical Physics, Courier Corporation, Russia.

25. Carslaw HS, Jaeger JC (1965) Conduction of heat in solids, Oxford University Press, UK.

26. Pankratov EL (2007) Dopant diffusion dynamics and optimal diffusion time as influenced by diffusion-coefficient nonuniformity. Russ Microelectron 36: 33-9.

27. Pankratov EL (2008) Redistribution Of A Dopant During Annealing Of Radiation Defects In A Multilayer Structure By Laser Scans For Production Of An Implanted-Junction Rectifier. Int J Nanoscience 7: 187-97.

28. Pankratov EL (2017) On Approach to Optimize Manufacturing of Bipolar Heterotransistors Framework Circuit of an Operational Amplifier to Increase Their Integration Rate. Influence Mismatch-Induced Stress. J Comp Theor Nano-science 14: 4885-99.

29. Pankratov EL (2017) On Optimization of Manufacturing of Two-Phase Logic Circuit Based on Heterostructures to Increase Density of Their Elements. Influence of Miss-Match Induced Stress. Adv Sci Eng Med 9: 787-801.

30. Pankratov EL, Bulaeva EA (2017) On increasing of density of transistors in a hybrid cascaded multilevel inverter. Multidiscipline Modeling in Materials and Structures 13: 664-77.

31. Pankratov EL, Bulaeva EA (2014) An approach to manufacture of bipolar transistors in thin film structures. On the method of optimization. Int J Micro-Nano Scale Transp 4: 17-31.

32. Pankratov EL, Bulaeva EA (2016) An analytical approach for analysis and optimization of formation of field-effect heterotransistors. Multidiscipline Modeling in Materials and Structures 12: 578-604.

33. Pankratov EL, Bulaeva EA (2015) An approach to increase the integration rate of planar drift heterobipolar transis-tors. Materials science in semiconductor processing 34: 260-8.

Submit your next manuscript to Annex Publishers and benefit from:

- Easy online submission process
- Rapid peer review process
- Online article availability soon after acceptance for Publication
- Open access: articles available free online
- More accessibility of the articles to the readers/researchers within the field
- Better discount on subsequent article submission

ANNEX PUBLISHERS Research

Submit your manuscript at
http://www.annexpublishers.com/paper-submission.php